Desalination and Water Treatment
www.deswater.com

doi: 10.1080/19443994.2015.1136693

57 (2016) 22618–22631
October

Taylor & Francis
Taylor & Francis Group

Synthesis of maghemite nanoparticles and its application for removal of Titan yellow from aqueous solutions using full factorial design

Ahmad Akrami, Ali Niazi*

Faculty of Science, Department of Chemistry, Arak Branch, Islamic Azad University, Arak, Iran, emails: a-niazi@iau-arak.ac.ir, ali.niazi@gmail.co (A. Niazi)

Received 29 April 2015; Accepted 8 December 2015

ABSTRACT

In this paper, batch adsorption experiments were carried out to investigate the maximum adsorption conditions of the anionic dye Titan yellow on maghemite nanoparticles (γ-Fe_2O_3). The γ-Fe_2O_3 nanoparticles were synthesized by co-precipitation method, and the γ-Fe_2O_3 nanoparticles structure was performed by transmission electronic microscopy, scanning electron microscope, XRD, and Brunauer–Emmett–Teller. The prepared magnetic adsorbent was well dispersed in water and easily separated magnetically from the medium after loaded with adsorbate. The main goal of this study was to analyze the role of experimental factors on the removal of Titan yellow from aqueous solution using full factorial design. The main and interactive effects of four most important variables like pH of the solution, dosage of adsorbent, initial concentration of dye, and contact time were investigated through the model equations designed by a two-level full factorial design. The results were statistically analyzed using the analysis of variance to define important experimental factors and their levels. A regression model that considers the significant main and interaction effects was suggested and fitted the experimental data very well. The optimized conditions for dye removal were at initial pH 6.0, 0.35 g L^{-1} of adsorbent, 30.0 mg L^{-1} dye, and 25.0 min adsorption time. The adsorption capacity was evaluated using both the Langmuir and Freundlich adsorption isotherm models. The maximum predicted adsorption capacities for Titan yellow was obtained as 839.421 mg g^{-1}. Furthermore, the kinetic of Titan yellow adsorption on γ-Fe_2O_3 nanoparticles was analyzed using pseudo-first- and second-order kinetic models and the results showed that the removal was mainly a pseudo-second-order process.

Keywords: Removal; Maghemite nanoparticles; Titan yellow; Full factorial design

1. Introduction

Dyes are one of the main categories of aquatic pollutants present in the effluents of many industries such as, additives, pulp and paper, solvent, printing, pesticide, paint, leathers- and wood-preserving chemicals [1]. Azo dyes (monoazo, diazo, triazo, and polyazo) are characterized by the presence of one or more azo bonds (–N≡N–) in association with one or more aromatic systems, which may also carry sulfonic acid groups [2]. Azo dyes, such as Titan yellow, are considered to be the largest chemical groups of dyes presently in existence (around 26,000 dyes) [3], and are the most common synthetic colorants released into the environment [4]. The release of azo dyes into the

*Corresponding author.

environment is of the main concern due to coloration of natural waters, toxicity, mutagenicity and carcinogenicity of the dyes and their biotransformation products [5]. Some dyes are reported to cause allergy, dermatitis, skin irritation, cancer, and mutations in humans [6]. Therefore, the removal of dyes from effluents is very important. Various techniques like coagulation/flocculation [7], photocatalytic degradation [8], ozonation [9], ion exchange [10], biological processes [11,12], and adsorption [13,14] have been examined for the removal of dyes from effluent. Adsorption process has been intensively concerned and found to be superior to another technique due to its low energy consumption, simple progress, and low cost [15]. Sorbent plays a key role in efficiently removal of dye from wastewater, so researcher's interest to focus on novel adsorbents that show high adsorption capacity. Different types of adsorbents like zeolite [16], chitosan [17], and activated carbon [18] have been investigated and used. Recently, nanometer-sized materials as novel adsorbents with their special properties have been developed by many researchers. The main attention has been paid to metal oxides like MnO_2 [19], Fe_3O_4 [20], and MgO [21]. In recent years, applications of magnetite and maghemite nanoparticles for removal of dye from aqueous solutions have received consideration [22–25]. Compared with micrometer-sized particles used in the adsorption method, the magnetic nanoparticles offer several advantages. Their high surface area provides higher adsorption capacity and their paramagnetic property grants rapid and easy collection of magnetic nanoparticles from samples by employing an external magnetic field. In this study, the γ-Fe_2O_3 nanoparticles were synthesized by co-precipitation technique and used as an adsorbent for the removal of Titan yellow from aqueous solutions. The isotherm of dye adsorption was studied in detail and the kinetic of Titan yellow adsorption on γ-Fe_2O_3 nanoparticles was analyzed using pseudo-first- and second-order kinetic models. The effects of operational parameters such as pH, adsorbent dosage, initial dye concentration, and contact time on dye removal were evaluated and optimized by full factorial design. The full factorial design was chosen in order to have an accurate study on the effects of each operational parameter and its interaction on depended variable(s) and improve the optimization process. Generally, full factorial design is suitable where dealing with multiple levels of several factors [26]. The number of experiments (N) required for the development of this design is defined as $N = 2^k$, where k is the factor number. The main goal of this paper was to investigate the adsorption capacity of the γ-Fe_2O_3 nanoparticles as an adsorbent for removal of the Titan yellow dye from aqueous solution. These particles showed the high adsorption capacity of Titan yellow.

2. Experimental

2.1. Instrumentation and software

The spectrophotometer (Hewlett-Packard 8453 diode array Agilent) which was controlled by a Hewlett-Packard computer and equipped with a 1-cm path length quartz cell was used for UV–visible spectra acquisition. A metrohm 691 pH-meter furnished with a combined glass-saturated calomel electrode was calibrated with at least two buffer solutions at pH 3.0 and 7.0. The size, morphology, and structure of the maghemite nanoparticles were characterized by transmission electronic microscopy (TEM, Philips, CM10, 100 kV) and scanning electron microscope (SEM, KYKY-EM3200). The XRD patterns of the synthesized products were obtained using an X-ray diffractometer (38,066 RIVA, d/G. Via M. Misone, 11/D (TN) Italy) at ambient temperature. The specific surface area was measured by the Brunauer–Emmett–Teller (BET) method using nitrogen adsorption–desorption isotherms on a Micrometrics ASAP 2020 system at 77 K. Design of the experiments and analysis of the results were done in MINITAB (Version 16). All programs were run on a personal computer with the Windows 7 operation system.

2.2. Chemicals and reagents

All the chemicals and reagents used in this work were of analytical grade. The stock solutions (1,000 mg L^{-1}) of Titan yellow (the structure was shown in Fig. 1) were prepared in double-distilled water and experimental solutions of their desired concentrations were obtained by successive dilutions of the stock solution with double-distilled water. Universal buffer solution was prepared by Lurie [27]. All laboratory glassware cleaned with a 5% (v/v) HNO_3 solution, and then rinsed with double-distilled water.

2.3. Synthesis of maghemite

The chemical co-precipitation method was used in the preparation of the γ-Fe_2O_3 nanoparticles. The maghemite nanoparticles were synthesized according to the method proposed elsewhere [28]. Briefly, 3.0 mL of $FeCl_3$ (2.0 mol L^{-1} dissolved in 2.0 mol L^{-1} HCl) was added to 10.33 mL of double-distilled water, and then 2.0 mL of Na_2SO_3 (1.0 mol L^{-1}) was added to the former solution dropwise in 1.0 min under magnetic

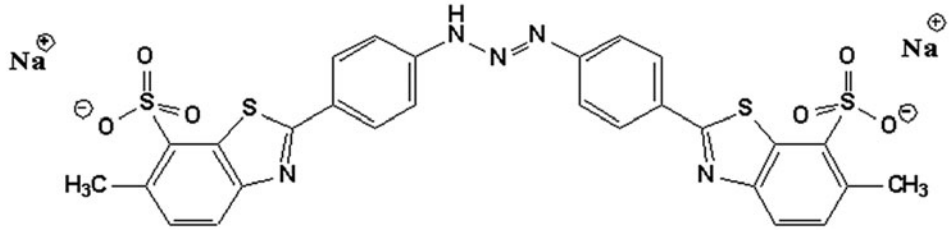

Fig. 1. Molecular structure of Titan yellow.

stirring. Just after mixing the solutions, the color of the solution changed from light yellow to red, indicating formation of complex ions between the Fe^{3+} and SO_3^{2-}. After turning the color of solution again, the solution was added to 80.0 mL of NH_3 solution (0.85 mol L^{-1}) under vigorous stirring. A black precipitate quickly formed, which was allowed to crystallize completely for another 30.0 min under magnetic stirring. The precipitate was washed with double-distilled water by magnetic decantation until the pH of the suspension was less than 7.5. A 170.0 mL water was added to this suspension and the pH of the suspension was adjusted to 3.0 with HCl (0.1 mol L^{-1}) and the pH was kept stable for 5.0 min. The suspension was refluxed under aeration (with air) for 60.0 min at about 100°C. The color of the suspension slowly changed from black to reddish-brown and the suspension became clear and transparent. The reddish-brown solution was washed with double-distilled water by magnetic decantation four times and the suspension was dried into powder.

2.4. General procedure

A batch procedure was applied for the adsorption studies of Titan yellow by maghemite nanoparticles (MNPs) at 25°C. Fifty milliliters of different concentrations of Titan yellow solutions that their pH value was adjusted to 6.0 with universal buffer were added to 0.018 g of MNPs in a glass beaker and the solutions were shaken for 30.0 min at 120.0 rpm. The concentration of Titan yellow decreased with time due to adsorption by MNPs. Nanoparticles were collected by an external magnetic field and the concentration of Titan yellow in the solution was then measured spectrophotometrically at 400 nm. The percent removal efficiency of Titan yellow was calculated using the following equation:

$$\%\,\text{Removal} = \frac{(C_0 - C_e)}{C_0} \times 100 \quad (1)$$

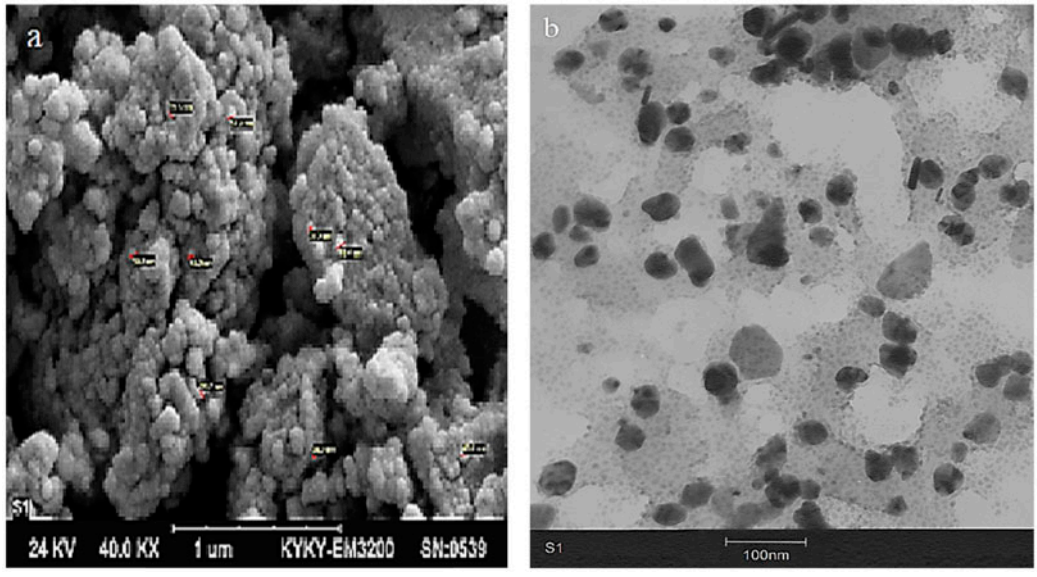

Fig. 2. SEM image (a) and TEM image (b) of γ-Fe_2O_3 NPs.

where C_0 (mg L^{-1}) is the initial concentration and C_e (mg L^{-1}) is the equilibrium concentration of the Titan yellow at 25°C. The effects of the experimental parameters to the adsorption capacity of MNPs in the experiments were investigated by full factorial design.

3. Results and discussion

3.1. Characterization of γ-Fe_2O_3 nanoparticles

Fig. 2 shows TEM and SEM images of the γ-Fe_2O_3 nanoparticles. As Fig. 2 shows, most of the nanoparticles have size around less than 100 nm. The XRD pattern of maghemite nanoparticles is shown in Fig. 3. The crystallite size of the maghemite nanoparticles measured around 9.86 nm from the XRD pattern according to Scherrer equation:

$$D = \frac{K\lambda}{b\cos\theta} \quad (2)$$

The equation uses the reference peak width at angle θ, where λ is the wavelength of incident X-ray (1.5418 Å), b is the width of the XRD peak at half height, and K is a shape factor, about 0.9 for magnetite and maghemite [29]. It should be noted that the particle dimension obtained by SEM is higher than the corresponding crystallite size, i.e. 9.86 nm. This difference may be explained due to the presence of aggregates in SEM grain consisting several crystallites and/or poor crystallinity [30]. The nitrogen adsorption and desorption isotherms for the maghemite nanoparticles are showed in Fig. 3. The specific surface area of maghemite nanoparticles, obtained by BET analysis, was 75.26 m^2 g^{-1}, and the mean pore diameter was 12.23 nm, with a total pore volume of 0.238 cm^3 g^{-1}. The isoelectric point can be used as a powerful tool to control the charge density of metal oxides by selecting the adequate pH. The MNPs surface is neutral at pH 6.3 [31]. The nanoparticles surface is negatively charged when the pH value is above pH 6.3 and is positively charged when the pH value is below it.

3.2. Optimization

The adsorption method of MNPs for Titan yellow was optimized under various conditions. Univariate procedure was employed to optimize important factors in this method. Optimal experimental parameters which affect the adsorption efficiency include pH, adsorbent dosage, initial concentration of Titan yellow, and contact time. These factors were optimized by full factorial design [26].

3.3. Effect of nanoparticles' amount

The amount of adsorbent is an important factor in adsorption method because it influences the recovery directly. Compared to ordinary sorbents (micro-sized sorbents), nanoparticles have higher surface areas. For this reason, fewer amounts of the adsorbent may achieve acceptable results because a significantly higher surface area-to-volume ratio. We studied the effect of the amount of nanoparticles on adsorption of 50.0 mL of 20.0 mg L^{-1} solution of Titan yellow at room temperature and pH 5.0, by varying the adsorbent amount from 0.01 to 0.024 g. As shown in Fig. 4, 0.018 g of MNPs was selected as the optimum amount

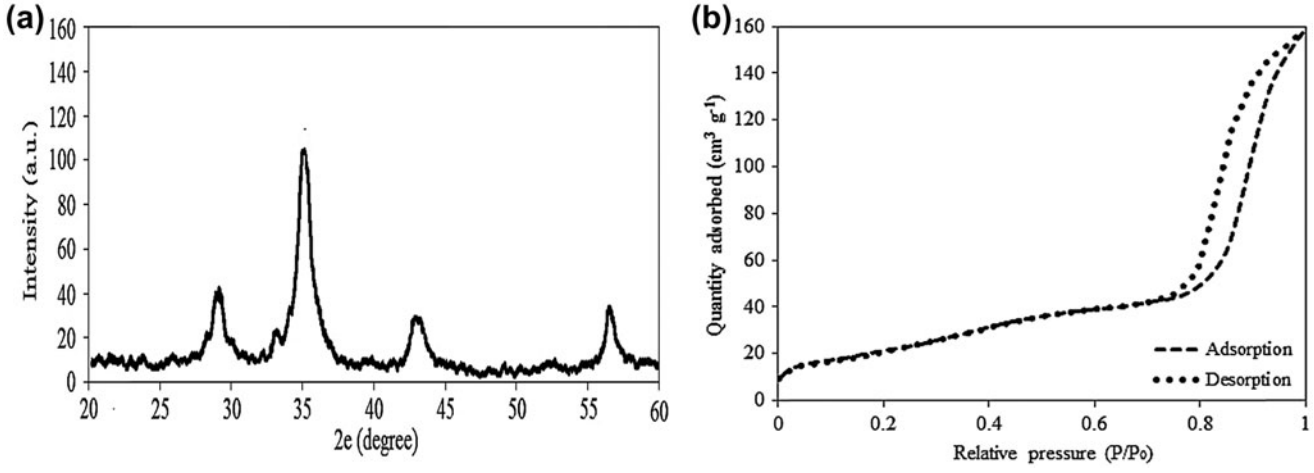

Fig. 3. XRD pattern (a) and nitrogen adsorption–desorption isotherms (b) of γ-Fe_2O_3 NPs.

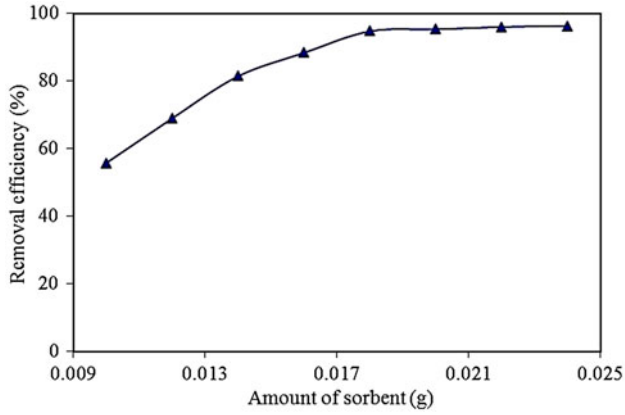

Fig. 4. Effect of the amount of the MNPs on the removal of Titan yellow, Conditions: sample's pH 5.0; 50.0 mL of 20.0 mg L^{-1} of Titan yellow; 20.0 min.

for further studies. According to the results, by increasing the amount of MNPs to 0.018 g, removal increases and stays constant afterward.

3.4. Effect of the pH sample

Among all parameters affecting on the removal, value of pH plays a critical role for adsorption of Titan yellow. The surfaces of metal oxides (γ-Fe_2O_3) are generally covered with hydroxyl groups that vary in forms at different pHs and play an important role in the positively and negatively charged nanoparticle. The surface charge is neutral at pH of zero point charge (pH_{zpc}) that for the maghemite nanoparticles is around 6.3 [31]. It is assumed here that negative charge is built up at the aqueous dispersed nanoparticle due to proton (H) transfer out from the nanoparticle surface toward the solvent. Thus, by starting at the zero point of charge and increasing the pH value in the aqueous medium, the chemisorbed proton (H) is assumed to move out from the nanoparticle surface (M–OH), leaving behind electron in the partially bonded oxygen atom (M–O). The electron left behind would be accommodated in the nanoparticle conduction band, while the surface oxygen atom is stabilized by a strongly bonded water layer around the nanoparticle surface. Such proton transfer mechanism results in a negative charge, which is mainly localized at the nanoparticle surface. In contrast, by starting at the zero point of charge and lowering the pH in the aqueous medium the available protons (H) are assumed to transfer from the acid solvent back to the nanoparticle surface, thus sets up a positive charge at the nanoparticle surface (M–OH) [32,33]. Therefore, adsorption of Titan yellow onto the adsorbent does take place. So, an appropriate pH value can improve the adsorption efficiency. The charge density of γ-Fe_2O_3 nanoparticles surface is a main factor affecting to removal of Titan yellow and its amount varies with the pH values. As mentioned before, the isoelectric point for γ-Fe_2O_3 nanoparticles is at pH of 6.3, so that below this pH value, maximum adsorption efficiency should be achieved. The effect of pH on the adsorption of Titan yellow with initial concentration of 20.0 mg L^{-1} over the pH range from 4.0 to 8.0 was studied. The adsorption percentage increased by increasing pH and reached a maximum at pH 6.0, and decreased at higher pH values. According to the results shown in Fig. 5, the maximum removal will be achieved at pH 6.0. Lower adsorption at pH values lower than 6.0 can be due to the dissolution of γ-Fe_2O_3 nanoparticles [34]. At higher pHs, the decrease in the positive charge of adsorbent surface sites can cause a decrease in the adsorption of Titan yellow.

3.5. Effect of contact time

In order to obtain an appropriate experimental time, the effect of the contact time on the removal of Titan yellow was investigated in the range of 10.0–45.0 min in samples with pH 6.0 and 0.018 g MNPs for 50.0 mL of 20.0 mg L^{-1} of Titan yellow. As it can be seen from Fig. 6, 30.0 min is needed for almost complete removal of Titan yellow. Hence, 30.0 min was selected as contact time for further works.

3.6. Effect of initial dye concentration

The adsorption of Titan yellow on the surfaces of MNPs is dependent to the initial concentrations of

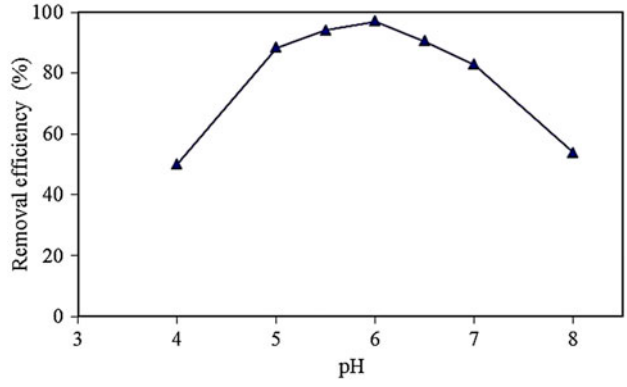

Fig. 5. Effect of sample's pH on the removal of Titan yellow, Conditions: 50.0 mL of 20.0 mg L^{-1} of Titan yellow; 0.018 g MNPs; 20.0 min.

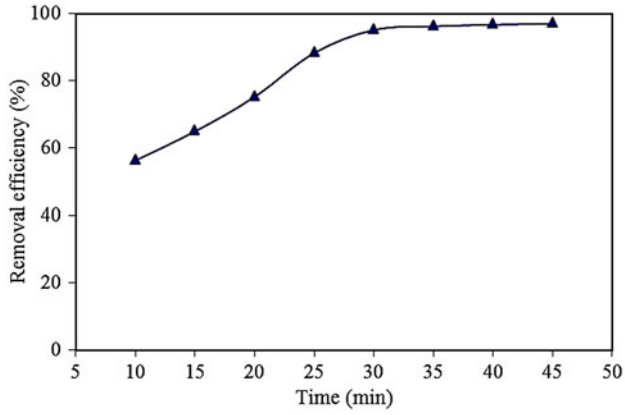

Fig. 6. Effect of contact time on the removal of Titan yellow, Conditions: sample's pH 6.0; 50.0 mL of 20.0 mg L^{-1} of Titan yellow; 0.018 g MNPs.

Titan yellow. So the effect of the initial Titan yellow concentration on the adsorption by MNPs was investigated at optimal condition in the range of 20–220 mg L^{-1} and the concentration of 30 mg L^{-1} was selected.

4. Experimental design

The classic optimization procedure varying "one variable at a time", is a method that does not guarantee the attainment of a true optimum of the experimental conditions, because the factors have an important effect on each other. Experimental design essentially is applicable for simultaneous optimization of the effects of variables to improve characteristics performance and minimize the errors. In present study, to investigate the influence of operating parameters, full factorial design was employed to determine the main effects as well as the interactive effects of the selected factors [35].

4.1. Full factorial design for multivariate optimization

Recently, the most widely used experimental design to evaluate the main effects, as well as interaction effects, is the full factorial design, where each variable is evaluated at two levels. In this study, four independent variables: solution pH (X_1), amount of MNPs (X_2), initial dye concentration (X_3), and time of contact (X_4) were chosen as important parameters, and removal efficiency (%) of Titan yellow was considered as a response. Notice that the factors used in this study have never been evaluated simultaneously and they were chosen for their importance, as determined previously using one-variable-at-a-time experimental procedures [36]. The number of experiments (N) required for the development of this design is defined as a^k where a is the number of levels and k is the number of factors. Totally, a full factorial design included $2^4 = 16$ experiments were run in this work to explore important factors and their interactions. Also, the center point of the design was replicated three times for the estimation of error. The experiments were executed in random manner order to correctly evaluate experimental errors [37]. Full factorial design matrix for real and coded values along with experimental and predicted values for removal efficiency (%) of Titan yellow by MNPs are shown in Table 1. Also, the experimental and predicted values for removal efficiency (%) of Titan yellow by MNPs under the different experimental combinations are shown in Fig. 7. The factor levels were coded as −1 (low), 0 (central point or middle) and +1 (high). Based on the experimental data, a first-degree polynomial model was established, which correlated the relationship between response and removal efficiency parameters. The relationship could be expressed by the following equation:

$$Y = \beta_0 + \beta_1 X_1 + \beta_2 X_2 + \beta_3 X_3 + \beta_4 X_4 + \beta_{12} X_1 X_2 + \beta_{13} X_1 X_3 + \beta_{14} X_1 X_4 + \beta_{23} X_2 X_3 + \beta_{24} X_2 X_4 + \beta_{34} X_3 X_4 + \beta_{123} X_1 X_2 X_3 + \beta_{124} X_1 X_2 X_4 + \beta_{134} X_1 X_3 X_4 + \beta_{234} X_2 X_3 X_4 + \beta_{1234} X_1 X_2 X_3 X_4 \quad (3)$$

where Y is a response variable of removal efficiency, β_0 is constant, β_1, β_2, β_3, β_4 and β_{12}, β_{13}, β_{14}, β_{23}, β_{24}, β_{34}, β_{123}, β_{124}, β_{134}, β_{234}, β_{1234} represent the regression coefficient corresponding to the main factor effects and interactions, respectively, which are estimated by the model and X_i represents independent variables: solution pH (X_1), amount of MNPs (X_2), initial dye concentration (X_3), and time of contact (X_4).

4.2. Analysis of variance

In order to evaluate the effect of the factors and their interactions, analysis of variance (ANOVA) was performed. ANOVA is a statistical technique that subdivides the total variation in a set of data into component parts associated with specific sources of variation for the purpose of testing hypotheses on the parameters of the model [38]. The statistical significance of the ratio of mean square variation due to regression and mean square residual error was tested using ANOVA. The results are listed in Table 2. As shown in Table 2, each factor that has p-value < 0.05 are

Table 1
Full factorial design matrix of real and coded values along with experimental and predicted values for removal efficiency (%) of Titan yellow by MNPs

		Levels				
Factors		Low (–1)	Central (0)	High (+1)		
X_1 pH		4.5	6	7.5		
X_2 Adsorbent dosage (g)		0.015	0.0175	0.02		
X_3 Titan yellow concentration (mg L^{-1})		15	30	45		
X_4 Contact time (min)		10	25	40	Removal efficiency (%)	
Run	X_1	X_2	X_3	X_4	Experimental	Predicted
1	−1	−1	−1	−1	61.98	62.33
2	+1	−1	−1	−1	58.39	57.66
3	−1	+1	−1	−1	72.25	71.47
4	+1	+1	−1	−1	61.32	61.77
5	−1	−1	+1	−1	54.23	54.22
6	+1	−1	+1	−1	48.33	48.72
7	−1	+1	+1	−1	63.05	63.35
8	+1	+1	+1	−1	52.78	52.83
9	−1	−1	−1	+1	70.65	70.49
10	+1	−1	−1	+1	61.68	61.60
11	−1	+1	−1	+1	77.15	77.74
12	+1	+1	−1	+1	63.46	63.83
13	−1	−1	+1	+1	58.33	58.15
14	+1	−1	+1	+1	56.45	56.87
15	−1	+1	+1	+1	65.51	65.41
16	+1	+1	+1	+1	59.96	59.10
17[a]	0	0	0	0	95.97	96.31
18[a]	0	0	0	0	96.32	96.31
19[a]	0	0	0	0	96.66	96.31

[a]Center point.

considered as potentially significant. The obtained results showed that all the factors (X_1, X_2, X_3, X_4, X_1X_2, X_1X_3, X_2X_4, and $X_1X_3X_4$) have a p-value of less than 0.05, indicating they are significant. Some terms which seem insignificant according to p-value were neglected. The reduced model which included the effects determined as "significant" in Table 2 is as follows:

$$Y = 61.596 - 3.799\,X_1 + 2.841\,X_2 - 4.265\,X_3 + 2.553\,X_4 - 1.256\,X_1\,X_2 + 0.848\,X_1\,X_3 - 0.469\,X_2\,X_4 + 1.055\,X_1\,X_3\,X_4 \quad (4)$$

A positive sign in the equation indicates an interactive effect of the variables, while a negative sign represents an antagonistic effect of the variables. The optimum values were obtained as follows: $\partial Y/\partial X_1$, $\partial Y/\partial X_2$, $\partial Y/\partial X_3$, and $\partial Y/\partial X_4$ were each equated to zero and the resulting three equation were solved simultaneously to obtain the values of X_1, X_2, X_3, and X_4 corresponding to maximum of Y. The optimum values of the tested parameters were obtained as follows: $X_1 = 6.0$, $X_2 = 0.35$ g L^{-1}, $X_3 = 30.0$ mg L^{-1}, and $X_4 = 25.0$ min. The adjusted R^2 is a useful tool for comparing the explanatory power of models with different numbers of predictors. This factor was used for choosing the model with the smallest mean square error [39]. The model presented an adjusted square correlation coefficient R^2 (adj) of 99.82%, fitting the statistical model quite well.

4.3. Main and interaction effects

The main effects of each parameter on the removal efficiency (%) are shown in Fig. 8. The main effects represent variations of the average between the high

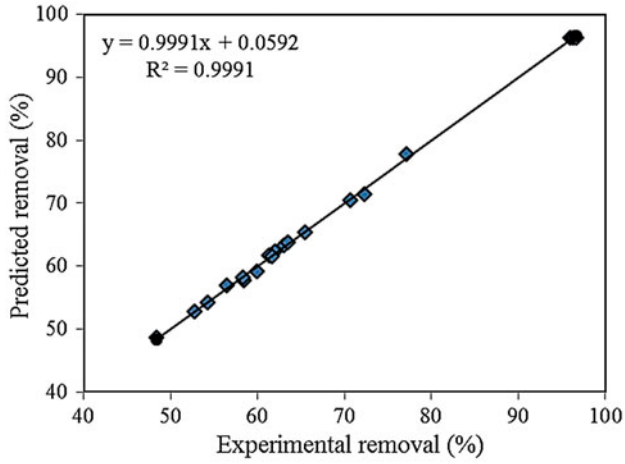

Fig. 7. Scatter diagram of predicted removal (%) vs. experimental removal (%) for the Titan yellow-MNPs adsorption system.

and low levels for each factor. If the slope is close to zero, then the magnitude of the main effect would be small. When the effect of a factor is positive, removal efficiency (%) increases as the factor changes from low to high levels. In contrast, if the effects are negative, a reduction in removal efficiency (%) happens for high level of the same factor. The interaction effect is effective when the change in the response from low to high levels of a factor is dependent on the level of a second factor. As shown in Fig. 9, if the lines of two factors are parallel, there is no interaction. In contrast, when the lines are not parallel, the two factors interact together.

4.4. The Pareto chart

Fig. 10 shows the Pareto chart of this design and demonstrates the important factors affected on removal efficiency (%). The significance of the factors and their interactions was determined by applying a Student's *t*-test with a 95% confidence interval. The values that exceed a reference line, i.e. those corresponding to the 95% confidence level, are significant values. The same results were obtained by plotting the probability normal plot (Fig. 10). Each point on the plot represents an effect. As shown in Fig. 11, the effects that are not statistically significant are located close to the reference line. The effects represented by points far from the reference line are considered statistically significant.

Table 2
Estimated regression coefficients of factors (coded units) and their effects for removal efficiency

Source	DF[a]	Effect	Coef	Adj SS	Adj MS	*F*-value	*p*-value	Remark
Main effects	4	–	61.596	755.34	188.83	1,585.83	0. 001	Highly significant
X_1	1	−7.598	−3.799	230.93	230.93	1,939.36	0.001	Highly significant
X_2	1	5.681	2.841	129.11	129.11	1,084.31	0. 001	Highly significant
X_3	1	−8.529	−4.265	290.99	290.99	2,443.76	0.000	Highly significant
X_4	1	5.106	2.553	104.30	104.30	875.90	0.001	Highly significant
2-way interaction	6	–	–	41.19	6.86	57.65	0.017	Significant
X_1X_2	1	−2.512	−1.256	25.24	25.24	211.97	0.005	Highly significant
X_1X_3	1	1.696	0.848	11.51	11.51	96.66	0.010	Highly significant
X_1X_4	1	0.074	0.037	0.02	0.02	0.19	0.708	
X_2X_3	1	0.312	0.156	0.39	0.39	3.26	0.213	
X_2X_4	1	−0.938	−0.469	3.52	3.52	29.57	0.032	Significant
X_3X_4	1	0.355	0.177	0.50	0.50	4.23	0.176	
3-way interactions	4	–		19.83	4.96	41.63	0.024	Significant
$X_1X_2X_3$	1	0.499	0.250	1.00	1.00	8.38	0.101	
$X_1X_2X_4$	1	0.413	0.207	0.68	0.68	5.73	0.139	
$X_1X_3X_4$	1	2.110	1.055	17.80	17.80	149.50	0.007	Highly significant
$X_2X_3X_4$	1	0.295	0.148	0.35	0.35	2.93	0.229	
4-Way Interactions	1	–	–	0.23	0.23	1.93	0.300	
$X_1X_2X_3X_4$	1	−0.239	−0.120	0.23	0.23	1.93	0.300	

[a]Degrees of freedom.

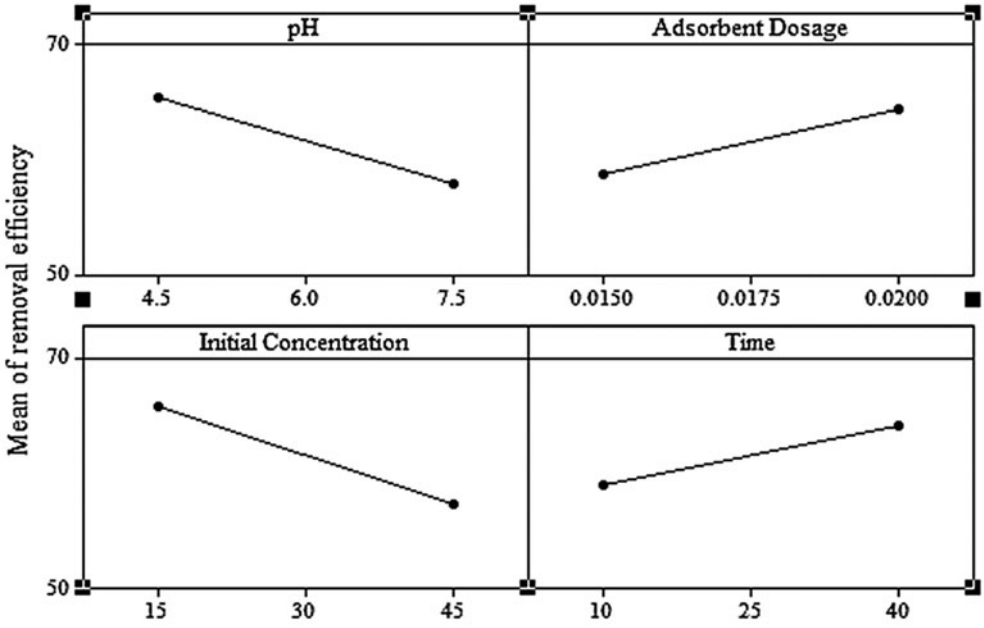

Fig. 8. Main effects plot for Titan yellow removal.

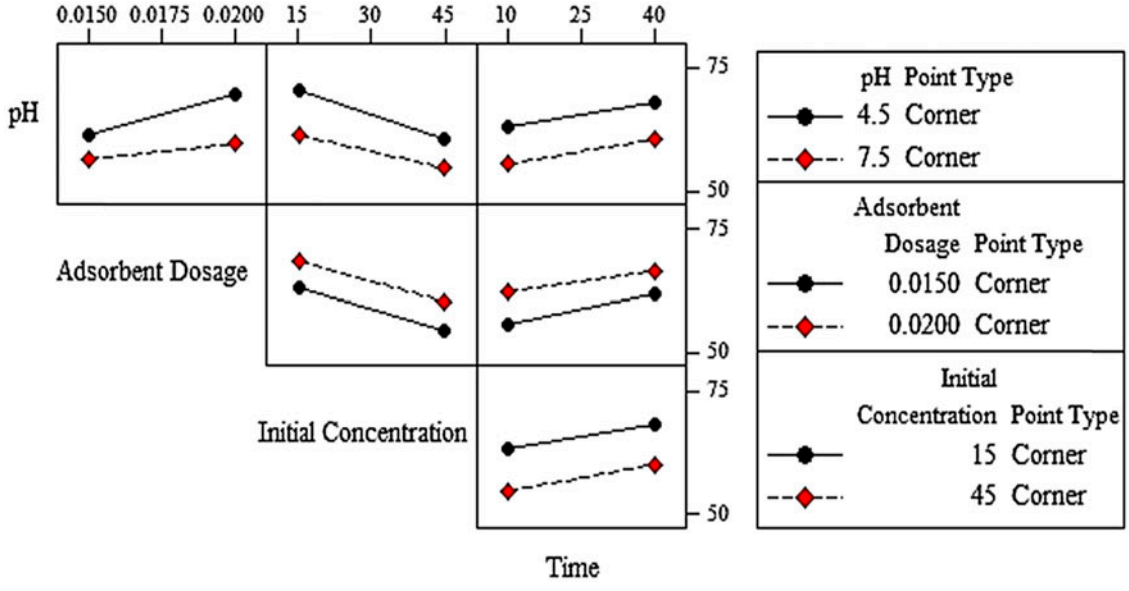

Fig. 9. Interaction effects plot for Titan yellow removal.

5. Adsorption isotherms

The equilibrium adsorption isotherm model describes the interactive behavior between adsorbate and adsorbent at constant temperature. In order to establish the most suitable correlation for the equilibrium data in the design of adsorption system, three most commonly isotherm models were tested: the Langmuir, Freundlich, and the Temkin models [40–42]. The main difference between these three isotherm models is in the variation of heat of adsorption with the surface coverage. Langmuir model assumes uniformity, Freundlich model assumes logarithmic decrease, and Temkin model assumes linear decrease in heat of adsorption with surface coverage [43]. Equilibrium isotherm studies were carried out with

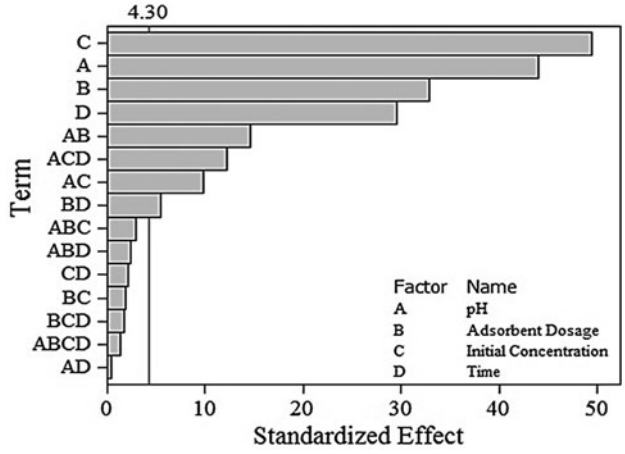

Fig. 10. Pareto chart of standardized effects of model variables.

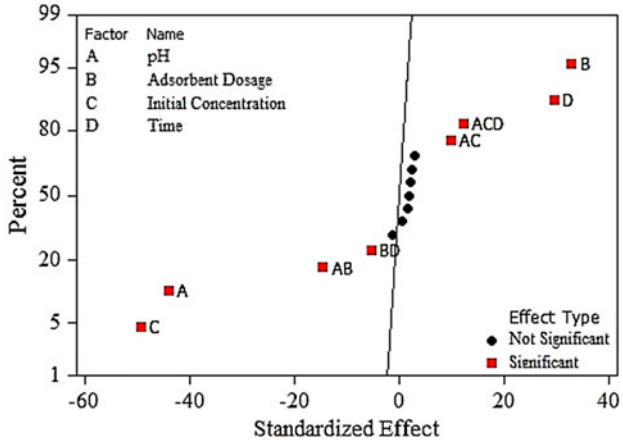

Fig. 11. Normal probability plot of standardized effects of model variables.

different initial concentrations of Titan yellow (20–680 mg L^{-1}) at 25°C and pH 6.0. The Langmuir isotherm model is based on the supposition that adsorption takes place on a homogenous surface by monolayer adsorption without interaction between adsorbate and the adsorbed material. The general form of the Langmuir isotherm is:

$$\frac{q_e a_L}{K_L} = \frac{K_L C_e}{1 + K_L C_e} \quad (5)$$

where C_e (mg L^{-1}) is the equilibrium concentration of the Titan yellow, q_e (mg g^{-1}) is the amount of Titan yellow adsorbed per unit mass of adsorbent, a_L (L mg^{-1}) and K_L (L g^{-1}) are the Langmuir constants with a_L related to the adsorption energy and q_m [$=K_L/a_L$] signifies the maximum adsorption capacity (mg g^{-1}), which depends on the number of adsorption sites. After linearization of the Langmuir isotherm, Eq. (6), we obtain:

$$\frac{C_e}{q_e} = C_e\left(\frac{a_L}{K_L}\right) + \left(\frac{1}{K_L}\right) \quad (6)$$

The values of a_L and K_L are calculated from the slope and intercept of the plot of C_e/q_e against the equilibrium concentration C_e (Fig. 12) and are presented in Table 3. The amount of Titan yellow adsorbed (mg g^{-1}) was calculated based on the mass balance equation which is given below:

$$q_e = \frac{V(C_0 - C_e)}{m} \quad (7)$$

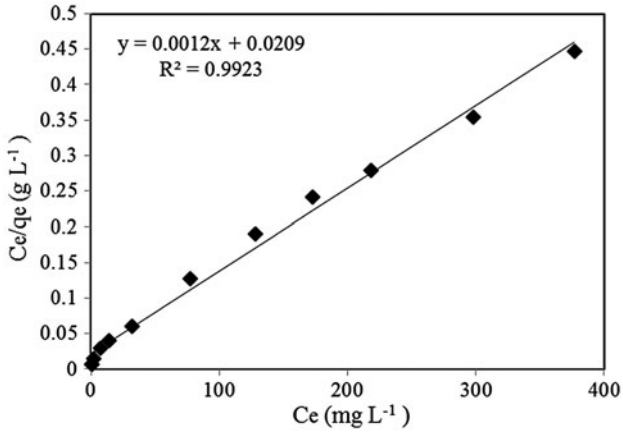

Fig. 12. Linearization of the Langmuir isotherm, Conditions: pH 6.0, 0.35 g L^{-1} MNPs, 25 min.

where C_0 is the initial concentration of Titan yellow in mg L^{-1}, V is the volume of experimental solution in L, and m is the dry weight of nanoparticles in g. The parameters of the Langmuir equation were calculated and are given in the Table 3. Table 3 indicates that the maximum adsorption capacity of maghemite nanoparticles for Titan yellow is 839.421 mg g^{-1}. As shown in Fig. 12, the adsorption obeys the Langmuir model. The R^2 value (0.992) suggests that the Langmuir isotherm provides a good fit to the isotherm data. The essential characteristics of the Langmuir isotherm can be expressed in terms of a dimensionless constant separation factor R_L [44] given by Eq. (8):

$$R_L = \frac{1}{(1 + a_L C_0)} \quad (8)$$

Table 3
Parameters of Langmuir, Freundlich and Temkin isotherm equations and regression coefficients (r) for the adsorption of Titan yellow on maghemite nanoparticles at 25℃ and at pH 6.0

Isotherm	Equation	Parameters	Value of parameters
Langmuir	$\frac{C_e}{q_e} = C_e\left(\frac{a_L}{K_L}\right) + \left(\frac{1}{K_L}\right)$	a_L (L mg^{-1})	0.057
		K_L (L g^{-1})	47.847
		K_L/a_L [=q_m] (mg g^{-1})	839.421
		R_L[a]	0.025
		r	0.992
Freundlich	$\ln q_e = \ln K_F + \left(\frac{1}{n}\right)\ln C_e$	K_F (mg$^{1-1/n}$ L$^{1/n}$ g^{-1})	119.546
		$1/n$	0.357
		r	0.981
Temkin	$q_e = B_1 \ln K_T + B_1 \ln C_e$	K_T (L mg^{-1})	3.707
		B_1	110.63
		b (J mol^{-1})	22.395
		r	0.953

[a]For Titan yellow concentration of 680 mg L^{-1}.

where C_0 (mg L^{-1}) is the highest initial concentration of adsorbent, and a_L (L mg^{-1}) is Langmuir constant. The R_L value of maghemite nanoparticles in the present study has been found to be 0.025 at 25℃ showing that the adsorption of Titan yellow is favorable at the studied temperature. The empirical Freundlich equation based on adsorption on a heterogeneous surface is given as follows, Eq. (9):

$$q_e = K_F C_e^{1/n} \tag{9}$$

where C_e is the equilibrium concentration (mg L^{-1}), q_e is the amount adsorbed at equilibrium (mg g^{-1}), K_F (mg$^{1-1/n}$ L$^{1/n}$ g^{-1}) and $1/n$ are Freundlich constants depending on the temperature and the given adsorbent–adsorbate couple. The n is related to the adsorption energy distribution, and K_F indicates the adsorption capacity. The linear form of Eq. (9) is:

$$\ln q_e = \ln K_F + \left(\frac{1}{n}\right)\ln C_e \tag{10}$$

The values of K_f and $1/n$ calculated from the intercept and slope of the plot of ln q_e against ln C_e and are listed in Table 3. The heat of the adsorption and the adsorbent–adsorbate interaction were studied by Temkin and Pyzhev [42], who suggested that because of these interactions the energy of adsorption of all the molecules decreases linearly with coverage. The Temkin isotherm has commonly been applied in the following form (11):

$$q_e = RT \ln K_T\left(\frac{C_e}{b}\right) \tag{11}$$

The Temkin isotherm Eq. (11) can be simplified to the following equation:

$$q_e = B_1 \ln K_T + B_1 \ln C_e \tag{12}$$

In this model, b is the Temkin constant related to the heat of sorption (J mol^{-1}) and K_T is the Temkin isotherm constant (L mg^{-1}), where $B_1 = (RT)/b$, T is the absolute temperature in Kelvin, and R is the universal gas constant, 8.314 J (mol K)$^{-1}$ [45,46]. The values of the Temkin constants and the correlation coefficient are listed in Table 3. A comparison of the correlation coefficient, r, values for the above three models indicate that the Langmuir model represents best the equilibrium isotherms tested in this work. The fact that the Langmuir isotherm fits the experimental data very well may be due to the homogenous distribution of active sites on the γ-Fe_2O_3 nanoparticles surface, since the Langmuir equation assumes that the surface is homogenous.

6. Adsorption kinetics

Kinetic modeling is important to know the nature of adsorption process. Kinetic studies provide important information about the mechanism of process; therefore, in order to determine the mechanism of adsorption, the removal of Titan yellow by γ-Fe_2O_3 nanoparticles was studied as a function of time and the results are shown in Table 4. After a specified interval of time equilibrium is reached, after that there is no change in the removal of Titan yellow. This phenomenon may be due to that at initial time, the numbers of available sites for adsorption are larger than

Table 4
Kinetic parameters and regression coefficients (r) for the adsorption of Titan yellow on maghemite nanoparticles at 25°C and at pH 6.0 ($q_{e(exp)}$ = 49.044 mg g^{-1})

Kinetics model	Equation	Parameters	Value of parameters
Pseudo-first-order	$\ln(q_e - q_t) = \ln(q_e) - k_1 t$	$q_{e(calc)}$ (mg g^{-1})	44.768
		K_1 (min^{-1})	8.750×10^{-2}
		r	0.991
Pseudo-second-order	$(t/q_t) = 1/k_2 q_e^2 + 1/q_e(t)$	$q_{e(calc)}$ (mg g^{-1})	63.291
		K_2 (g (mg min)$^{-1}$)	1.470×10^{-3}
		r	0.995

close to equilibrium. Kinetic modeling creates the information for this equilibrium time and the mechanism of adsorption. The adsorption data at various contact times (5, 10, 15, 20, 25, 30 min) with constant dose of adsorbent 0.018 g, pH 6.0 and concentration 20.0 mg L^{-1} were analyzed by pseudo-first-order and pseudo-second-order kinetic models [47,48]. A simple kinetic model that describes the process of adsorption is the pseudo-first-order equation. The pseudo-first-order rate equation is given as (in the transformed logarithmic form):

$$\ln(q_e - q_t) = \ln(q_e) - k_1 t \quad (13)$$

where q_e and q_t are the amounts of Titan yellow adsorbed (mg g^{-1}) at equilibrium and at time (min), respectively, and k_1 (min^{-1}) is the adsorption rate constant of first-order adsorption. The straight line of the plot of $\ln(q_e - q_t)$ vs. time suggests the applicability of this kinetic model. The values of rate constant, k_1 and q_e together with regression coefficients are provided in Table 4. The experimental data were also fitted to the pseudo-second-order kinetic model Eq. (14):

$$(t/q_t) = 1/k_2 q_e^2 + 1/q_e(t) \quad (14)$$

where k_2 is the rate constant of pseudo-second-order chemisorption (g (mg min)$^{-1}$). According to Eq. (14), the plot t/q_t vs. time should be a straight line with a slope $1/q_e$. The values of q_e, k_2, and r were determined by the intercept and the slope of the plot and are given in Table 4. As shown in Table 4, the correlation coefficient value for pseudo-second-order model is higher than that of pseudo-first-order model and suggesting that the adsorbent systems is well described by the pseudo-second-order kinetic model.

7. Desorption and reusability studies

In this study, the desorption of Titan yellow from the γ-Fe_2O_3 NPs was studied using different solvents including sodium hydroxide solution (0.1 mol L^{-1}), sodium chloride solution (0.1 mol L^{-1}), pure methanol, and ethanol. In order to desorb Titan yellow from the γ-Fe_2O_3 NPs, 0.01 g Titan yellow-loaded maghemite nanoparticle was mixed with 5 mL of different solvents and the desorption efficiency for them was calculated. The adsorbed Titan yellow could be desorbed in the presence of sodium hydroxide solution (0.1 mol L^{-1}) with 95% removal efficiency. Hence, Titan yellow could be desorbed from the loaded nanoparticles by changing the pH of the solution to alkaline range and NaOH solution (0.1 mol L^{-1}) has higher desorption efficiency compared to the other eluents.

8. Conclusion

This study demonstrates that γ-Fe_2O_3 nanoparticles by high adsorption capacity and with easy separation of maghemite nanoparticles are so good candidate for removal of dye from aqueous solutions. The effect of different parameters e.g. solution pH, biomass dosage, dye concentration, and contact time were studied for the removal of Titan yellow by γ-Fe_2O_3. Experimental design technique carried out using two-level full factorial design to avoid the classic one-factor-at-a-time experiments. A high correlation coefficient (R^2 = 99.91%, adjusted R^2 = 99.82%) ensured the satisfactory adjustment of the proposed model to the experimental data. Statistical tools such as ANOVA and F-test were used to define the most important process variables affecting the removal efficiency (%).The adsorption isotherm data for the Titan yellow were derived at room temperature and treated according to Langmuir, Freundlich, and Temkin models. Langmuir model is almost more successful in representing experimental isotherm data for the adsorption of Titan yellow on maghemite nanoparticles than the

Freundlich and Temkin models. A pseudo-second-order kinetic model agreed well with the dynamical behavior for the adsorption of Titan yellow on γ-Fe_2O_3 nanoparticles under different temperatures.

Acknowledgments

The authors gratefully acknowledge the support to this work from, Islamic Azad University, Arak Branch, and research council.

References

[1] G. Crini, P.M. Badot, Application of chitosan, a natural aminopolysaccharide, for dye removal from aqueous solutions by adsorption processes using batch studies: A review of recent literature, Prog. Polym. Sci. 33 (2008) 399–447.
[2] P. Tripathi, V.C. Srivastava, A. Kumar, Optimization of an azo dye batch adsorption parameters using Box–Behnken design, Desalination 249 (2009) 1273–1279.
[3] S.V. Mohan, N.C. Rao, J. Karthikeyan, Adsorptive removal of direct azo dye from aqueous phase onto coal based sorbents: A kinetic and mechanistic study, J. Hazard. Mater. 90 (2002) 189–204.
[4] K. Selvam, K. Swaminathan, K.-S. Chae, Decolourization of azo dyes and a dye industry effluent by a white rot fungus Thelephora sp, Bioresour Technol. 88 (2003) 115–119.
[5] Y.M. Kolekar, S.P. Pawar, K.R. Gawai, P.D. Lokhande, Y.S. Shouche, K.M. Kodam, Decolorization and degradation of Disperse Blue 79 and Acid Orange 10, by *Bacillus fusiformis* KMK5 isolated from the textile dye contaminated soil, Bioresour. Technol. 99 (2008) 8999–9003.
[6] H. Keharia, D. Madamwar, Bioremediation concepts for treatment of dye containing waste water: A review, Indian J. Exp. Biol. 41 (2003) 1068–1075.
[7] P.C. Vandevivere, R. Bianchi, W. Verstraete, Review: Treatment and reuse of wastewater from the textile wet-processing industry: review of emerging technologies, J. Chem. Technol. Biotechnol. 72 (1998) 289–302.
[8] M. Sleiman, D. Vildozo, C. Ferronato, J.M. Chovelon, Photocatalytic degradation of azo dye Metanil Yellow: Optimization and kinetic modeling using a chemometric approach, Appl. Catal. B: Environ. 77 (2007) 1–11.
[9] A. Baban, A. Yediler, D. Lienert, N. Kemerdere, A. Kettrup, Ozonation of high strength segregated effluents from a woollen textile dyeing and finishing plant, Dyes Pigm. 58 (2003) 93–98.
[10] Y. Yu, Y.Y. Zhuang, Z.H. Wang, Adsorption of water-soluble dye onto functionalized resin, J. Colloid Interface Sci. 242 (2001) 288–293.
[11] S. Sirianuntapiboon, O. Sadahiro, P. Salee, Some properties of a granular activated carbon-sequencing batch reactor (GAC-SBR) system for treatment of textile wastewater containing direct dyes, J. Environ. Manage. 85 (2007) 162–170.
[12] M. Işık, D.T. Sponza, Anaerobic/aerobic treatment of a simulated textile wastewater, Sep. Purif. Technol. 60 (2008) 64–72.
[13] S. Allen, B. Koumanova, Decolourisation of water/wastewater using adsorption, J. Univ. Chem. Technol. Metal. 40 (2005) 175–192.
[14] Y. Al-Degs, M.A.M. Khraisheh, S.J. Allen, M.N.A. Ahmad, Sorption behavior of cationic and anionic dyes from aqueous solution on different types of activated carbons, Sep. Sci. Technol. 36 (2001) 91–102.
[15] C.R.T. Tarley, M.A.Z. Arruda, Biosorption of heavy metals using rice milling by-products. Characterisation and application for removal of metals from aqueous effluents, Chemosphere 54 (2004) 987–995.
[16] A. Faki, M. Turan, O. Ozdemir, A.Z. Turan, Analysis of fixed-bed column adsorption of reactive yellow 176 onto surfactant-modified zeolite, Ind. Eng. Chem. Res. 47 (2008) 6999–7004.
[17] S. Chatterjee, S. Chatterjee, B.P. Chatterjee, A.K. Guha, Adsorptive removal of congo red, a carcinogenic textile dye by chitosan hydrobeads: Binding mechanism, equilibrium and kinetics, Colloids Surf., A: Physicochem. Eng. Aspects 299 (2007) 146–152.
[18] R. Jain, V.K. Gupta, S. Sikarwar, Adsorption and desorption studies on hazardous dye Naphthol Yellow S, J. Hazard. Mater. 182 (2010) 749–756.
[19] J.B. Fei, Y. Cui, X.H. Yan, W. Qi, Y. Yang, K.W. Wang, Q. He, J.B. Li, Controlled preparation of MnO_2 hierarchical hollow nanostructures and their application in water treatment, Adv. Mater. 20 (2008) 452–456.
[20] L.S. Zhong, J.S. Hu, H.P. Liang, A.M. Cao, W.G. Song, L.J. Wan, Self-assembled 3D flowerlike iron oxide nanostructures and their application in water treatment, Adv. Mater. 18 (2006) 2426–2431.
[21] G. Moussavi, M. Mahmoudi, Removal of azo and anthraquinone reactive dyes from industrial wastewaters using MgO nanoparticles, J. Hazard. Mater. 168 (2009) 806–812.
[22] Z. Tang, Y. Chen, J. Xue, S. Yue, Adsorption and removal of congo red dye from aqueous solution by using nano-Fe_3O_4, Adv. Mater. Res. 503–504 (2012) 262–265.
[23] M. Roosta, M. Ghaedi, N. Shokri, A. Daneshfar, R. Sahraei, A. Asghari, Optimization of the combined ultrasonic assisted/adsorption method for the removal of malachite green by gold nanoparticles loaded on activated carbon: Experimental design, Spectrochim. Acta Part A: Mol. Biomol. Spectrosc. 118 (2014) 55–65.
[24] A. Afkhami, R. Moosavi, Adsorptive removal of Congo red, a carcinogenic textile dye, from aqueous solutions by maghemite nanoparticles, J. Hazard. Mater. 174 (2010) 398–403.
[25] K.P. Singh, S. Gupta, A.K. Singh, S. Sinha, Experimental design and response surface modeling for optimization of Rhodamine B removal from water by magnetic nanocomposite, Chem. Eng. J. 165 (2010) 151–160.
[26] D.C. Montgomery, Design and Analysis of Experiments, John Wiley & Sons, New York, 1997.
[27] J.J. Lurie, Handbook of Analytical Chemistry, Mir Publishers, Moscow, 1987.
[28] Y.K. Sun, M. Ma, Y. Zhang, N. Gu, Synthesis of nanometer-size maghemite particles from magnetite, Colloids Surf. A 245 (2004) 15–19.
[29] J. Hu, G. Chen, I.M.C. Lo, Removal and recovery of Cr(VI) from wastewater by maghemite nanoparticles, Water Res. 39 (2005) 4528–4536.

[30] R.N. Panda, M.F. Hsieh, R.J. Chung, T.S. Chin, FTIR, XRD, SEM and solid state NMR investigations of carbonate-containing hydroxyapatite nano-particles synthesized by hydroxide gel technique, J. Phys. Chem. Solids 64 (2003) 193–199.
[31] R. Han, D. Ding, Y. Xu, W. Zou, Y. Wang, Y. Li, L. Zou, Use of rice husk for the adsorption of congo red from aqueous solution in column mode, Bioresour. Technol. 99 (2008) 2938–2946.
[32] Q. Fanyaou, P.C. Morais, The pH dependence of the surface charge density in oxide-based semiconductor nanoparticles immersed in aqueous solution, IEEE Trans. Magn. 37 (2001) 2654-2656.
[33] P.C. Morais, Q. Fanyao, A quantum dot model for the surface charge density in ferrite-based ionic magnetic fluids, J. Magn. Magn. Mater. 252 (2002) 117–119.
[34] A. Afkhami, R. Norooz-Asl, Removal, preconcentration and determination of Mo(VI) from water and wastewater samples using maghemite nanoparticles, Colloids Surf., A: Physicochem. Eng. Aspects 346 (2009) 52–57.
[35] C. Gonçalves, J.J. Carvalho, M.A. Azenha, M.F. Alpendurada, Optimization of supercritical fluid extraction of pesticide residues in soil by means of central composite design and analysis by gas chromatography–tandem mass spectrometry, J. Chromatogr. A 1110 (2006) 6–14.
[36] E. Guibal, Interactions of metal ions with chitosan-based sorbents: A review, Sep. Purif. Technol. 38 (2004) 43–74.
[37] G.P.G. Box, J.S. Hunter, W.G. Hunter, Statistics for Experimenters: Design Innovation and Discovery, John Wiley & Sons, New York, 2005.
[38] L. Huiping, Z. Guoqun, N. Shanting, L. Yiguo, Technologic parameter optimization of gas quenching process using response surface method, Comput. Mater. Sci. 38 (2007) 561–570.
[39] S. Alizadeh, M. Kordkandi, Forouzesh, Application of full factorial design for methylene blue dye removal using heat-activated persulfate oxidation, J. Taiwan Inst. Chem. Eng. 45 (2014) 2597–2604.
[40] I. Langmuir, The adsorption of gases on plane surfaces of glass, mica and platinum, J. Am. Chem. Soc. 40 (1918) 1361–1403.
[41] H. Freundlich, W. Heller, The adsorption of cis - and trans-azobenzene, J. Am. Chem. Soc. 61 (1939) 2228–2230.
[42] M.J. Tempkin, V. Pyzhev, Recent modifications to langmuir isotherms, Acta Physiol. Chem. USSR 12 (1940) 217–222.
[43] B.H. Hameed, A.T.M. Din, A.L. Ahmad, Adsorption of methylene blue onto bamboo-based activated carbon: Kinetics and equilibrium studies, J. Hazard. Mater. 141 (2007) 819–825.
[44] E. Bulut, M. Özacar, İ.A. Şengil, Equilibrium and kinetic data and process design for adsorption of Congo Red onto bentonite, J. Hazard. Mater. 154 (2008) 613–622.
[45] A. Fakhri, Investigation of mercury (II) adsorption from aqueous solution onto copper oxide nanoparticles: Optimization using response surface methodology, Process Saf. Environ. Prot. 93 (2015) 1–8.
[46] A. Fakhri, S. Behrouz, Comparison studies of adsorption properties of MgO nanoparticles and ZnO–MgO nanocomposites for linezolid antibiotic removal from aqueous solution using response surface methodology, Process Saf. Environ. Prot. 94 (2015) 37–43.
[47] L.A. Al-Khateeb, A.Y. Obaid, N.A. Asiri, M. Abdel Salam, Adsorption behavior of estrogenic compounds on carbon nanotubes from aqueous solutions: Kinetic and thermodynamic studies, J. Ind. Eng. Chem. 20 (2014) 916–924.
[48] A. Fakhri, S. Adami, Adsorption and thermodynamic study of Cephalosporins antibiotics from aqueous solution onto MgO nanoparticles, J. Taiwan Inst. Chem. Eng. 45 (2014) 1001–1006.